[C_nC_1im][NTF_2] (n = 1, 2, … 8) İyonik Sıvılarında Elektronik Yapı, Spektroskopik Özellikler ve İyonlar Arası Zayıf Etkileşmelerin Alkali Zincir Uzunluğuna Bağlılığının İncelenmesi

Fehmi BARDAK

Manisa Celal Bayar Üniversitesi, Fizik Bölümü, Manisa

e-posta: fehmi.bardak@cbu.edu.tr

Özet

Anahtar kelimeler
İyonik sıvı; DFT; TD-DFT; Zayıf etkileşme analizi; Nano yapısal organizasyon

Bu çalışmada, [C_nC_1im][NTf_2][1-alkyl-3-methylimidazolium bis(trifluoromethylsulfonyl)imide] (n = 1, 2, … 8) için değişen alkali zincir uzunluğuna göre elektronik yapı, bazı fiziksel ve optik özelliklerin değişimi yoğunluk fonksiyonu teorisi (DFT) metotları kullanarak teorik olarak incelendi. Geometrik yapı ve frekans hesaplamaları popülasyon analizi ile birlikte DFT-B3LYP/6-311G(d,p) teori ve baz seti kullanılarak yapıldı. İndirgenmiş yoğunluk değişimleri analizi yapılarak iyon içi ve iyonlar arası hidrojen bağlanmaları ve van der Waals etkileşmeleri görüntülendi. Etkileşmelerin yoğun olduğu bölgeler için geometrik yapı ve titreşimsel özellikleri analiz edilerek nano yapısal organizasyonla ilişkisi araştırıldı. Becke yüzeyi ve Hirsfeld analizi temel alınarak iyonlar arası etkileşmelerin karakteristikleri tanımlandı. Elektronik geçiş özellikleri zamana bağlı yoğunluk fonksiyonu teorisi kullanılarak incelendi. Soğurma spektrumları ile iyonik sıvılarda zincir uzunluğuna bağlı olarak gözlenen renk değişimlerinin sebebi açıklandı.

Investigation of Dependence of Electronic Structure, Spectroscopic Features, and Interionic Weak Interactions on Alkyl Chain Length in [C_nC_1im][NTF_2] (n=1,2, .. 8) Ionic Liquids

Abstract

Keywords
Ionic liquid; DFT; TD-DFT; Weak Interaction analysis; Nano structural organization

In this work, electronic structure and some physical and optical properties [C_nC_1im][NTf_2][1-alkyl-3-methylimidazolium bis(trifluoromethylsulfonyl)imide] (n = 1, 2, ... 8) were investigated theoretically via density functional theory calculations within the dependency of alkyl chain length. Geometrical structure and frequency calculations along with population analysis were performed at DFT-B3LYP/6-311G(d,p) level of theory. Inter- and intra-molecular hydrogen bonding and van der Waals interactions were visualized by using reduced density gradient analysis. Geometrical structure and vibrational features were analyzed in detail for the strong interaction regions, and their relation to nano structural organization was explored. Characteristics of interionic interactions were fingerprinted on the basis of Becke surface and Hirshfeld analysis. Electronic transition properties were investigated by time dependent density functional theory. The reason for colored appearance comes with elongation of chain length is explained through absorbance spectra.

1. Introduction

Room-temperature ionic liquids (RT-ILs) are molten salts that are liquids at or below 100^0 C (Plechkova and Seddon 2008). They differ from common molten salts in terms of the temperature regime where they are liquids and in terms of their lower viscosity. Inorganic (single, non-complexing) molten salts are liquid in the 300 to 600 ^{0} C range whereas the ILs can be liquid at temperatures as low as -96 ^{0} C. The first realized unique qualities of ILs were their dissolving capacity, negligible vapor pressure, thermal stability, and electrochemical

window (Tokuda, et al. 2004; Tokuda, et al. 2005). Some well-known applications that stem from above mentioned characteristics of ILs are CO_2 capture/activation and subsequent conversion (Camper, et al. 2008; Yang, et al. 2011b), stabilization of proteins (Klahn, et al. 2011; Kumar and Venkatesu 2014; Rawat and Bohidara 2015; Satish, et al. 2016; Weingartner, et al. 2012), biomass processing (Schutt, et al. 2017; Wang, et al. 2012), novel solvents for chemical extraction and separation (Abbasian, et al. 2017; Tang, et al. 2012), electrolytes for batteries, super-capacitors, and dye-sensitized solar cells (Ohno 2011; Shvedene, et al. 2008; Wishart 2009), the desulfurization of transportation fuels (Kulkarni and Afonso 2010), and nuclear fuel processing (James and Ilya 2009). The field of ILs, actually, experienced a breakthrough with the synthesis of imidazolium based ILs by Wilkes and Zaworotko in 1992 (Wilkes and Zaworotko 1992) who found these ILs to be relatively air and water stable.

Imidazolium-based ILs are also the most widely studied systems in experiments and computations in terms of their structure and dynamics (Chew, et al. 2017; Khakan and Yeganegi 2017; Wu, et al. 2016; Zhou, et al. 2017). The ILs studied in this work are in the same group. A typical ion pair of [methyl imidazolium bis(trifluoromethane)sulfonamide], $[C_nC_1im][NTf_2]$, with group definitions is given in Figure 1. The cation in these ILs is often investigated in two parts as a positively charged head group (imidazolium ring) and a non-polar tail (alkyl chain).
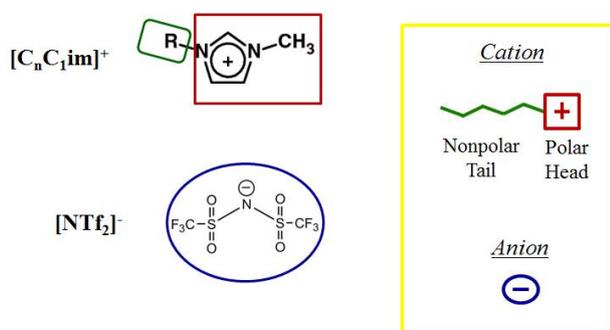

Figure 1: Group definitions for $[C_nC_1im][NTf_2]$ ionic liquids

Imidazolium-based ILs with more than four carbons in their alkyl chains were observed to have a nano structural organization by the aggregation of alkyl chains forming nonpolar domains and the charge ordering of ionic parts forming a three-dimensional ionic network in the liquid state. Additionally, the size of these heterogeneous regions is proportional to the length of the alkyl chain (Urahata and Ribeiro 2005; Wang and Voth 2005). To establish the chain length dependency of nano structural heterogeneities, Lopes and Padua (Canongia Lopes and Pádua 2006) performed a fully atomistic model to investigate a series of ILs with 1-alkyl-3-methyl imidazolium cation and $[PF_6]^-$ and $[NTf_2]^-$ anions. This heterogeneous structure picture has also been proven experimentally by using x-ray diffraction studies by Triolo*et al.* (Triolo, et al. 2007), in neutron diffraction measurements by Deetlefs *et al.* (Deetlefs, et al. 2006), and in optical heterodyne-detected Raman-induced Kerr effect spectroscopy (OHD-RIKES) studies of Quitevis and coworkers (Russina, et al. 2009; Xiao, et al. 2009; Xiao, et al. 2007).

Here we focus on understanding the intrinsic reasons for nano structural organization in $[C_nC_1im][NTf_2]$ (n = 1, 2, ... 8) ILs and interionic interactions profile that varies depending on the alkyl chain length. Some studies already suggest that multiple hydrogen bonding occur between ion pairs by considering only the distances between atoms. However, it is not very satisfactory to address this issue by only geometrical interpretations. Although, we also investigate the geometry of single molecules to have a first idea about possibly highly interacting regions, we interpret the nature of interionic interactions. These regional interactions are based on three powerful intermolecular interaction analysis methods: reduced density gradient, Hirshfeld, and Becke surface analysis. Then, some reasonable connections between nano structural organization, interaction profile, and spectroscopic features of single molecules were established.

2. Material and Methods

2.1 Computational Details

All calculations were carried out by using Gaussian 09 software (Frisch, et al. 2009). Molecular structure, molecular orbitals, calculated spectra, and surfaces and counters were visualized in Gauss view 5.0 (Roy Dennington 2009). It has been known by experience that the utilization of the gradient corrected density functional theory (DFT) with the Becke's three-parameter hybrid functional (B3) for the exchange part and the Lee-Yang-Parr (LYP) correlation function is a cost effective approach to obtain satisfactory results in the calculation of molecular structure, frequencies, and related thermochemical functions (Karabacak, et al. 2008; Shoba, et al. 2011; Swaminathan, et al. 2010). To estimate the best molecular wave function guess, 6-311 Gaussian combination for the core and shell molecular orbitals, d polarization for the C and N atoms and p polarization for the H atoms were combined. Thus, DFT B3LYP/6-311G(d,p) level of theory used in optimization and frequency calculations with full population analysis and nonlinear optical properties. The electronic properties were determined via TD-DFT calculations at the same level of theory.

2.2 Weak Interaction Analysis

Non-covalent interactions were obtained mapping the reduced density gradient (RDG)

$$s(\boldsymbol{r}) = \left[1 \Big/ 2(3\pi^2)^{1/3} \right] \Big/ \left[|\nabla\rho(\boldsymbol{r})| \Big/ \rho(\boldsymbol{r})^{4/3} \right]$$
(1)

onto the $\rho(\boldsymbol{r}).\text{sign}(\lambda_2)$ quantity as suggested by Johnson *et al.* (Sarangi, et al. 2010) using Multiwfn 3.3.6 (Lu and Chen 2012). Visualization of these interactions in a color coded pattern was produced in VMD (Humphrey, et al. 1996) program.

2.3 Hirshfeld and Becke surface analyses

The main purpose of these analyses is to obtain the inter-fragmental interactions and differentiate the hydrogen bonding interactions from van der Waals (vdW) interactions (Spackman and Byrom 1997; Spackman and Jayatilaka 2009). Atomic Hirshfeld weighting function of an atom is given by

$$w_A^{Hirsh}(\boldsymbol{r}) = \frac{\rho_A^0(\boldsymbol{r})}{\sum_B \rho_A^0(\boldsymbol{r})} \quad (2)$$

where $\rho_A^0(\boldsymbol{r})$ denotes the density of atom A in free-state. Hirshfeld weight of the fragment (anion or cation in our case) is then written as

$$w_P^{Hirsh}(\boldsymbol{r}) = \sum_{A \in P} w_A^{Hirsh}(\boldsymbol{r}) \quad (3)$$

Hirshfeld surface of fragment *P* is just the isosurface of $w_P^{Hirsh}(\boldsymbol{r}) = 0.5$. In the case of Becke surface analysis, Becke weighting function is used instead (Becke 1988). Using Hirshfeld surface analysis, a unique real space function normalized contact distance can be defined as

$$d_{norm} = \frac{d_i - r_i^{vdW}}{r_i^{vdW}} + \frac{d_e - r_e^{vdW}}{r_e^{vdW}} \quad (4)$$

where d_i and d_e are distances from a point on the surface to the nearest nucleus inside and outside, r_i^{vdW} and r_e^{vdW} are the vdW radiuses of the corresponding two atoms. Intermolecular contact points, thus, can be determined by the small values of d_{norm}. A plot of d_i versus d_e, named fingerprint plot, produces a pair of peaks for each hydrogen bonding type interactions and the color coding indicates the strength of interactions (Spackman and McKinnon 2002).

3. Results and Discussions

3.1. Geometrical structure and vibrational spectra

Optimized structures of $[C_nC_1im][NTf_2]$ (n = 1, 2, … 8) ILs calculated DFT B3LYP/6-311G(d,p) level of theory are presented in Figure 2.
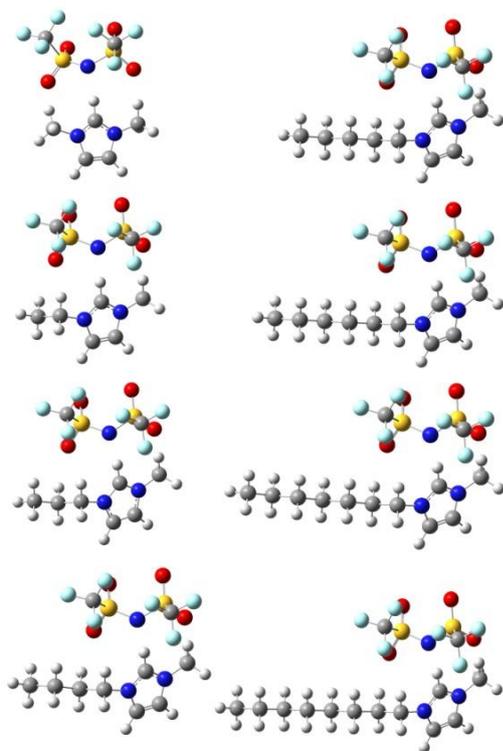

Figure 2: Optimized geometrical structures

There is not any significant variation in the structure of anion in any case. Actually, $[NTf_2]^-$ anion has *cis* and *trans* geometry in isolated form, and *trans* form is lower in energy. In the case of *trans* form, trifluorosulfonate groups are in asymmetric positions. This configuration of anion, though, causes weaker interionic interactions because more electronegative sections of anion are further away from the polar head of the cation. Therefore, the anion is always considered in *cis* form. Nonpolar tail in cations elongates linearly without any significant bending. The most essentially expected interionic interactions which can have impact on the structure of ILs are hydrogen bindings and vdW interactions. Possible regions for these interactions to occur are the region between nitrogen of anion and hydrogen on the near side of the ring, the region between methyl group on the polar head and the oxygen in

anion, and any other interaction might occur between the anion and hydrogens on tail. Our interest is to answer the questions of what are the types of these interactions, do they multiply exist, and how these interactions vary with increase in chain length. Table 1 summarizes bond length parameters for critical regions in cation, anion, and interionic region depending on the increase in chain length.

$r_{\text{Head C−H}}$, expected to experience a strong potential because of just being at the center of interionic region, is not varied significantly with the change in the chain length. $r_{\text{Head 1 C−H}}$, parameters belong to methyl group remains unchanged. A clear dependency on the chain length is observed in $r_{C−H}$ of tail end methyl group parameters; it increases with increasing number of carbons on the chain up to fourth carbon then remains the same. This is a very meaningful result in terms of nano structural organizational nature observed in these ILs. According to experimental results from small & wide angle X-ray scattering data (Triolo, et al. 2007), and optical Kerr effect spectroscopy results (Xiao, et al. 2007; Xiao, et al. 2008; Yang, et al. 2011a), and theoretical explanations brought out by molecular dynamic simulation studies (Canongia Lopes and Pádua 2006) nano structural organization is observed in imidazolium based ILs with n = 4 or more. ILs with longer tail thus separated into two distinct, polar and nonpolar, regions. This situation is true for the bulk state of the material as well as for the individual molecular scale. The hydrogens in tail are under influence of a strong potential due to interionic interactions in shorter sections of the tail, and the hydrogens in further carbons are affected by much weaker external forces.

Table 1 : Variations in bond lengths for critical regions in cation, anion, and interionic region depending on the increase in chain length

Bond lengths (Å)	n=1	n=2	n=3	n=4	n=5	n=6	n=7	n=8
Cation								
Head C-H	1.0931	1.0931	1.0924	1.0923	1.0924	1.0923	1.0921	1.092
Head 1 C-H	1.0896	1.0901	1.0896	1.0896	1.0897	1.0896	1.0905	1.0897
Tail 1 C-H	1.0894	1.0877	1.0884	1.0882	1.0882	1.0884	1.0883	1.0883
Tail 2 C-H		1.0899	1.092	1.0927	1.0926	1.0926	1.0924	1.0925
Tail 3 C-H			1.0919	1.0972	1.0982	1.0981	1.0951	1.095
Tail 4 C-H				1.0927	1.0956	1.0966	1.0965	1.0965
Tail End C-H					1.0938	1.0942	1.0943	1.0944
Anion								
Head N-S	1.6234	1.6237	1.624	1.6236	1.6236	1.6236	1.6237	1.6235
Tail N-S	1.6198	1.6174	1.6193	1.6189	1.6179	1.6184	1.6184	1.6182
Head S-O	1.4682	1.467	1.4679	1.4679	1.4677	1.4678	1.468	1.468
Tail S-O	1.4684	1.4685	1.4678	1.4678	1.4677	1.4675	1.4675	1.4675
Intermolecular								
N-H	1.9692	1.963	1.9717	1.9734	1.9653	1.9692	1.9695	1.9675
Head O-H	2.0945	2.0921		2.1119	2.117	2.1161	2.1237	2.1249
Tail O-H				2.4163	2.4371	2.4499	2.4689	2.4565

Interestingly, the bond lengths in anion remain unchanged as the cation varies from $[C_1C_1im]^+$ to $[C_8C_1im]^+$. The bond angles or dihedral angles also do not change depending on variation in chain length. This is due to $[NTf_2]^-$ anion consisting of highly electronegative atoms which makes the intramolecular interactions strong, thus not to be affected by interionic interactions.

Intermolecular bond lengths recorded here are basically between the nitrogen of anion and hydrogen in head group, and oxygens of anion and hydrogen of head methyl group or first chain of tail. These parameters are commonly taken as hydrogen bonding; however it is not safe to decide by only interpretation of bond lengths. Remaining parts of our study strictly focuses on addressing this issue.

From the perspective of nano structural organization, the tail part should be isolated from polar network; however it cannot be a sharp transition. IR and Raman spectra of ILs are given in Figure 3 shows that ν_{C-H} stretching bands (given as inset) varies depending on the chain length. The shift in the peak position to lower frequency (nearly 40 cm^{-1}) is a result of weakening of the external potential.

Vibrational wavenumbers corresponding to each peak were also analyzed. Frequencies of anion do not change as its geometrical parameters. Vibrations show slight deviations are only the methyl group vibrations either on the head or end of tail. Intermolecular vibrations also show some deviations, but they are more like fluctuations among ILs without any meaningful order.
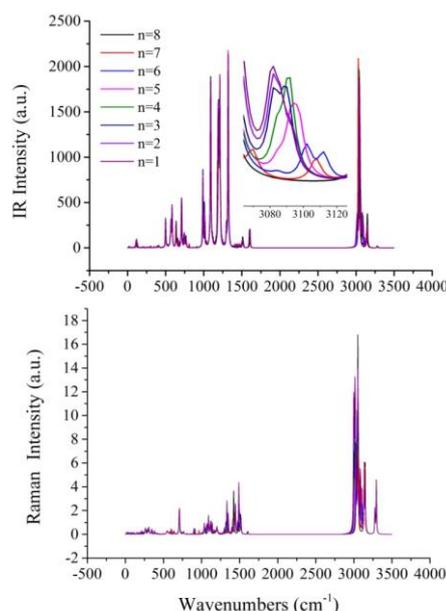
Figure 3: IR and Raman spectra obtained from DFT calculations.

3.2. Interionic interaction analysis

1185

A very intuitive way of analyzing the results of quantum chemistry calculations is to use the reduced density gradient (RDG) analysis. Through this analysis, the weak interactions such as hydrogen bonding, vdW, π-π, and dispersion interactions other than covalent bonding can be visualized clearly. As introduced by Johnson *et al.*(Johnson, et al. 2010), RDG is a dimensionless quantity measuring the deviation of electron density from uniform electron gas. These interaction types can be visualized using VMD program and color mapped as the strongest repulsions are represented with red and the strongest attractions are represented with blue and mild interactions are colored depend on their strength. Figure 4 shows a steric effect at the center of imidazolium ring and multiple complex interactions between ions. There are also some strong intramolecular interactions appears in $[NTf_2]^-$ anion. The strongest interionic interaction occurs clearly between nitrogen of anion and the hydrogen on the ring which was resulted in average bond length of 1.9686 Å. Interactions between the anion and hydrogens of second and further carbons of the tail are vdW interactions. The type of interactions between oxygens of anion and the hydrogens in methyl group in polar head side and the hydrogen in the first carbon on tail is not clear.
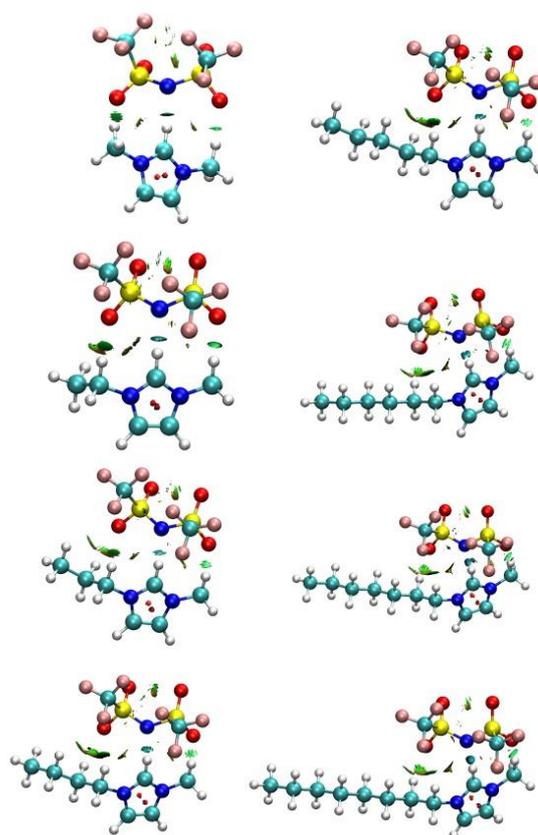

Figure 4: The color map of weak interactions

We used two more interfacial region orientated methodology to analyze the interfacial region between ions. Figure 5 shows the visualization of Becke surfaces in red-green-blue scale. In these figures, left side shows the methyl group-anion interfacial region, and right side shows that of tail-anion as oppose to molecular configuration given in Figure 2. Blue spots clearly exist on each surface indicate a strong hydrogen bonding between ions. This is an expected outcome according to results of geometrical analysis. Geometrical parameters in Table 1 indicate some bonding between in other regions, and RDG analysis leave a grey area for interpretation on the type of these interactions. Becke surface analysis clarifies this issue with a quite clear visualization. This analysis brings out a well determination of vdW interactions as well. $[C_1C_1im][NTf_2]$ has only two distinct vdW interactions with very near intensity. The interaction in methyl group-anion interfacial region is always strong. On the other hand, the vdW interactions in anion-tail interface are modified in $[C_2C_1im][NTf_2]$; a second slight green spot starts to appear and the fist spot becomes

weaker. The second vdW interaction becomes more distinctive after [C$_3$C$_1$im][NTf$_2$] and remains same for the longer chain ILs. The interfacial interaction profile for the ILs with n=4 or more, thus, is the same.
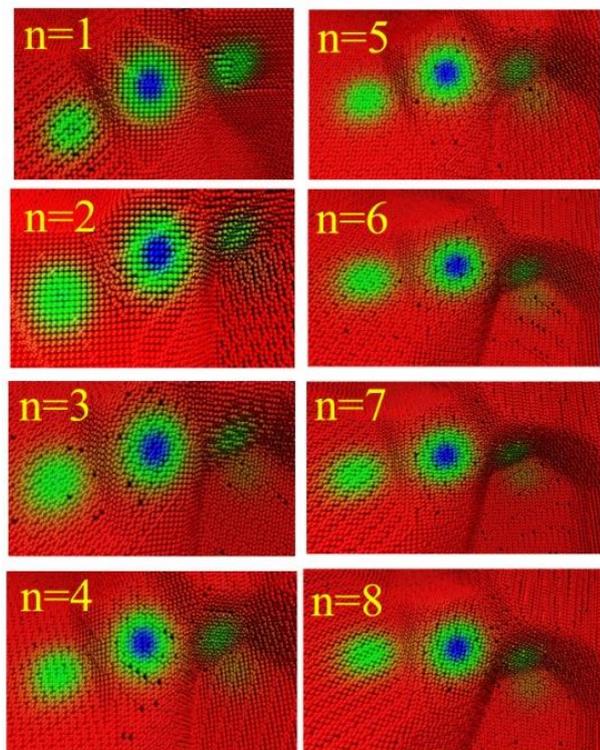

Figure 5: Becke surfaces representing the interfacial region between ions

Although, the color coding in Becke surface analysis is powerful in separation between different types of interactions, there is still some user dependency in determination of color scale. To overcome this ambiguity, we employed fingerprint analysis for interionic interactions. Fingerprint analysis assign a peak pair for each hydrogen bonding and gives the intensity of vdW interaction in color scale. Figure 6 shows the fingerprint plot of [C$_n$C$_1$im][NTf$_2$] ILs. In these figures, x and y axes correspond to d_i and d_e, respectively (See Section 2.3 for details). It can be seen that there is only one pair of peaks in all plots, strictly suggesting occurrence of a single hydrogen bonding between ions. The lower peak is at $d_i = 1.18 > d_e = 0.80$ and higher peak is at $d_i = 1.8 > d_e = 0.9$ shows that the hydrogen bonding occurs between N-H (Maloney, et al. 2014; McKinnon, et al. 2007; McKinnon, et al. 2004). Fingerprint analysis indicates that strength

of interactions in [C$_1$C$_1$im][NTf$_2$] is significantly weaker than that of any other IL, and the coloring of the plots are the same for all remaining ILs. This shows that although the fingerprint analysis is very powerful in determination in number of hydrogen bonds, not very promising in analysis of vdW interactions.
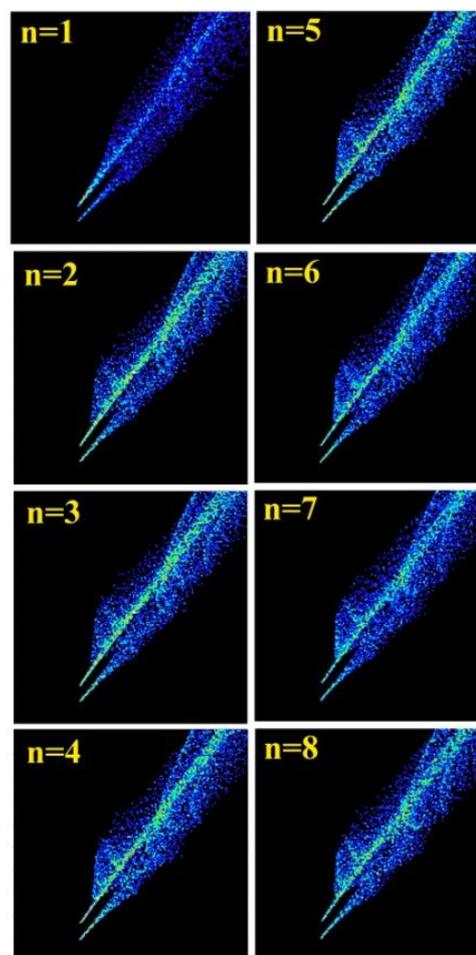

Figure 6: Fingerprint analysis of intermolecular interactions

3.3. Electronic structure properties and colors

Optical and spectroscopic applications require no color in ILs while some other usage of ILs in photovoltaics or electrochemical industries benefit from their color. Therefore, it is a critical issue to define their electronic structure properties that are related to their color nature. On the other hand, some ILs expected to be colorless show some slight yellowish color which is a problematic issue in spectroscopic applications (Earle, et al. 2006). This slight color results in an extension of absorption spectra to the wavelengths longer than 400 nm in experimental

UV-Vis spectra. Some cases, this extension resides as a significant background that indicates the color observed may results from impurities in the liquids. Figure 7 shows TD-DFT calculation results on UV spectral characteristics of title ILs. y-axis is specifically given as logarithmic to scale up the near zero extension part of the spectra. First of all, UV spectra of all ILs looks same except that of $[C_5C_1im][NTf_2]$. The reason for this deviation cannot be explained within the content of this study; it requires a deeper analysis on density of states and molecular orbital composition. Nevertheless, none of UV spectra extends to visible region, thus indicating that any color might be observed in these ILs are not due to their nature but rather from impurities.
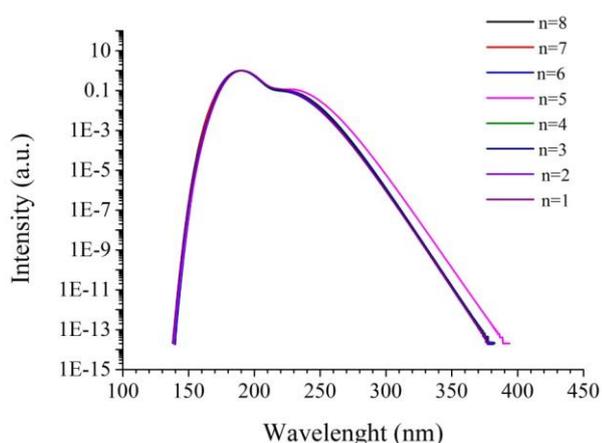

Figure 7: Calculated UV spectra

The relation between the electronic structure and the alkyl chain length is also observed in evaluation of HOMO-LUMO band gaps. As can be seen in Table 2, $\Delta E = E_{LUMO} - E_{HOMO}$ values decreases on going from $[C_1C_1im][NTf_2]$ to $[C_3C_1im][NTf_2]$, then remains the same for any longer chain IL. Similar trend was observed in the Becke surface analysis.

Table 2: Dependency of HOMO, LUMO, and ΔE energies on the chain length

Chain Length	HOMO (eV)	LUMO (eV)	ΔE (eV)	ΔE (nm)
n=1	-7.55	-1.60	5.95	208.38
n=2	-7.54	-1.53	6.01	206.30
n=3	-7.55	-1.50	6.05	204.90
n=4	-7.54	-1.48	6.06	204.60
n=5	-7.54	-1.48	6.06	204.60
n=6	-7.54	-1.48	6.06	204.60
n=7	-7.53	-1.47	6.06	204.60
n=8	-7.53	-1.47	-6.06	204.60

4. Conclusions

Geometrical structure, vibrational characteristics, intermolecular interactions, and electronic absorption properties of $[C_nC_1im][NTf_2]$ (n = 1, 2, ... 8) ILs were investigated through DFT and TD-DFT/B3LYP-6311G(d,p) quantum calculations within the dependency on the alkyl chain length. The variations in bond lengths and vibrational frequencies for the interfacial region and the tail end show a well agreement to nano structural nature of these ILs. Through a complementary and intuitive analysis of intermolecular interactions via RDG, Becke surface, and fingerprint analyses, existence of a single hydrogen bonding between ions and multiple vdW interactions is proven. The slight color observed in $[C_nC_1im][NTf_2]$ in bulk state is most likely due to impurities and not a result of intrinsic property of them.

References

Abbasian M., Balali-Mood M., Amoli H.S., and Masoumi A., 2017. A new solid-phase microextraction fiber for separation and determination of methamphetamines in human urine using sol-gel technique. *Journal of Sol-Gel Science and Technology*, **81(1),** 247-260.

Becke, A. D., 1988. A multicenter numerical integration scheme for polyatomic molecules. *The Journal of Chemical Physics*, **88(4),** 2547-2553.

Camper D., Bara J.E., Gin D. L. and Noble R.D., 2008. Room-Temperature Ionic Liquid–Amine Solutions: Tunable Solvents for Efficient and Reversible Capture of CO2. *Industrial & Engineering Chemistry Research*, **47(21),** 8496-8498.

Chew, E. K., Lee K. Y., and Lau E. V., 2017. The role of carbon chain length in the attachment between microbubbles and aqueous solutions of ionic liquid. *Journal of Colloid and Interface Science*, **506,** 452-459.

Deetlefs M., Hardacre C., Nieuwenhuyzen M., Padua A.A.H., Sheppard O., and Soper A.K., 2006. Liquid Structure of the Ionic Liquid 1,3-Dimethylimidazolium Bis{(trifluoromethyl)sulfonyl}amide. *The Journal of Physical Chemistry B*, **110(24),** 12055-12061.

Dennington R., Keith T., and Millam J., 2009. GaussView. *In* Semichem Inc., Vol. Version 5.

Earle M.J., Gordon C.M., Plechkova N.V., Seddon K.R., and Welton T., 2006. Decolorization of Ionic Liquids for Spectroscopy. *Analytical Chemistry*, **79(2),** 758-764.

Gaussian 09, Revision A.02, M. J. Frisch, G. W. Trucks, H. B. Schlegel, G. E. Scuseria, M. A. Robb, J. R. Cheeseman, G. Scalmani, V. Barone, G. A. Petersson, H. Nakatsuji, X. Li, M. Caricato, A. Marenich, J. Bloino, B. G. Janesko, R. Gomperts, B. Mennucci, H. P. Hratchian, J. V. Ortiz, A. F. Izmaylov, J. L. Sonnenberg, D. Williams-Young, F. Ding, F. Lipparini, F. Egidi, J. Goings, B. Peng, A. Petrone, T. Henderson, D. Ranasinghe, V. G. Zakrzewski, J. Gao, N. Rega, G. Zheng, W. Liang, M. Hada, M. Ehara, K. Toyota, R. Fukuda, J. Hasegawa, M. Ishida, T. Nakajima, Y. Honda, O. Kitao, H. Nakai, T. Vreven, K. Throssell, J. A. Montgomery, Jr., J. E. Peralta, F. Ogliaro, M. Bearpark, J. J. Heyd, E. Brothers, K. N. Kudin, V. N. Staroverov, T. Keith, R. Kobayashi, J. Normand, K. Raghavachari, A. Rendell, J. C. Burant, S. S. Iyengar, J. Tomasi, M. Cossi, J. M. Millam, M. Klene, C. Adamo, R. Cammi, J. W. Ochterski, R. L. Martin, K. Morokuma, O. Farkas, J. B. Foresman, and D. J. Fox, Gaussian, Inc., Wallingford CT, 2016. Humphrey, William, Andrew Dalke, and Klaus Schulten 1996. VMD: Visual molecular dynamics. *Journal of Molecular Graphics*, **14(1),** 33-38.

Hermann W., Cabrele C., and Herrmann C., 2012. How ionic liquids can help to stabilize native proteins. *Physical Chemistry Chemical Physics*, **14(2),** 415-426.

Hiroyuki O., 2011. Electrochemical Aspects of Ionic Liquids, 2nd Edition. New York: Wiley.

Johnson E.R., Keinan S., Mori-Sánchez P., Contreras-García P., Cohen A.J. and Yang W., 2010. Revealing Noncovalent Interactions. *Journal of the American Chemical Society*, **132(18),** 6498-6506.

Karabacak M., Karagöz D., and Kurt M., 2008. Experimental (FT-IR and FT-Raman spectra) and theoretical (ab initio HF, DFT) study of 2-chloro-5-methylaniline. *Journal of Molecular Structure*, **892(1–3),** 25-31.

Khakan, H., and Yeganegi S., 2017. Molecular Dynamics Simulations of Amide Functionalized Imidazolium Bis(trifluoromethanesulfonyl)imide Dicationic Ionic Liquids. *Journal of Physical Chemistry B*, **121(31),** 7455-7463.

Klahn, M., G. S. Lim, and P. Wu 2011. How ion properties determine the stability of a lipase enzyme in ionic liquids: A molecular dynamics study. *Physical Chemistry Chemical Physics*, **13(41),** 18647-18660.

Kulkarni, P. S., and Carlos A. M. A., 2010. Deep desulfurization of diesel fuel using ionic liquids: current status and future challenges. *Green Chemistry*, **12(7),** 1139-1149.

Kumar, A., and Venkatesu P., 2014. The stability of insulin in the presence of short alkyl chain imidazolium-based ionic liquids. *RSC Advances*, **4(9),** 4487-4499.

Lopes C., José N. A., and Pádua A.A.H., 2006. Nanostructural Organization in Ionic Liquids. *The Journal of Physical Chemistry B*, **110(7),** 3330-3335.

Maloney, A. G. P., Wood A.P., and Parsons S., 2014. Competition between hydrogen bonding and dispersion interactions in the crystal structures of the primary amines. *CrystEngComm*, **16(19),** 3867-3882.

McKinnon, J.J., Spackman M.A., and Mitchell A.S., 2004. Novel tools for visualizing and exploring intermolecular interactions in molecular crystals. *Acta Crystallographica Section B*, **60(6),** 627-668.

McKinnon, J.J., Jayatilaka D., and Mark A. S., 2007. Towards quantitative analysis of intermolecular interactions with Hirshfeld surfaces. *Chemical Communications*, **(37),** 3814-3816.

Nagabalasubramanian P.B., Karabacak M., Periandy S., 2010. FT-IR, FT-Raman, ab initio and DFT structural and vibrational frequency analysis of 6-aminopenicillanic acid. *Spectrochimica Acta Part A: Molecular and Biomolecular Spectroscopy*, **75(1),** 183-190.

Plechkova, N.V., and Seddon K.R., 2008. Applications of ionic liquids in the chemical industry. *Chemical Society Reviews*, **37(1),** 123-150.

Rawat, K. and Bohidara H. B., 2015. Heparin-like native protein aggregate dissociation by 1-alkyl-3-methyl imidazolium chloride ionic liquids. *International Journal of Biological Macromolecules*, **73,** 23-30.

Russina O., Triolo A., Gontrani L., Caminiti R., Xiao D., Hines L.G.Jr, Bartsch R.A, Quitevis E.L., Plechkova N. and Seddon K.R., 2009. Morphology and intermolecular dynamics of 1-alkyl-3-methylimidazolium bis{(trifluoromethane)sulfonyl}amide ionic liquids: structural and dynamic evidence of nanoscale segregation. *Journal of Physics: Condensed Matter*, **21(42)**.

Sarangi S.S., Zhao W., Müller-Plathe F., Balasubramanian S., 2010. Correlation between dynamic heterogeneity and local structure in a room-temperature ionic liquid: a molecular dynamics study of [bmim][PF(6)]. *ChemPhysChem*, **11(9),** 2001-10.

Satish L., Rana S., Arakha M., Rout L., Ekka B., Jha S., Dash P. Sahoo H., 2016. Impact of imidazolium-based ionic liquids on the structure and stability of lysozyme. *Spectroscopy Letters*, **49(6),** 383-390.

Schutt T.C., Hegde G.A., Bharadwaj V.S., Johns A.J., Maupin C.M., 2017. Impact of Water-Dilution on the Solvation Properties of the Ionic Liquid 1-Methyltriethoxy-3-ethylimidazolium Acetate for Model Biomass Molecules. *Journal of Physical Chemistry B*, **121(4),** 843-853.

Shoba D., Periandy S., Karabacak M., Ramalingam S., 2011. Vibrational spectroscopy (FT-IR and FT-Raman) investigation, and hybrid computational (HF and DFT) analysis on the structure of 2,3-naphthalenediol. *Spectrochimica Acta Part A: Molecular and Biomolecular Spectroscopy*, **83(1),** 540-552.

Shvedene, N. V., Chernyshov D. V., and Pletnev I. V., 2008. Ionic liquids in electrochemical sensors. *Russian Journal of General Chemistry*, **78(12),** 2507-2520.

Spackman, M. A., and Byrom P.G., 1997. A novel definition of a molecule in a crystal. *Chemical Physics Letters*, **267(3–4),** 215-220.

Spackman, M.A. and Jayatilaka D., 2009. Hirshfeld surface analysis. *CrystEngComm*, **11(1),** 19-32.

Spackman, M.A., and McKinnon J.J., 2002. Fingerprinting intermolecular interactions in molecular crystals. *CrystEngComm*, **4(66),** 378-392.

Tang B., Bi W., Tian M., Row K.H., 2012. Application of ionic liquid for extraction and separation of bioactive compounds from plants. *Journal of Chromatography B*, **904(0),** 1-21.

Tian L., and Chen F., 2012. Multiwfn: A multifunctional wavefunction analyzer. *Journal of Computational Chemistry*, **33(5),** 580-592.

Tokuda H., Hayamizu K., Ishii K., Susan A.B.H. , and Watanabe M., 2004. Physicochemical properties and structures of room temperature ionic liquids. 1. Variation of anionic species. *Journal of Physical Chemistry B*, **108(42),** 16593-16600.

Tokuda H., Hayamizu K., Ishii K., Susan A.B.H. , and Watanabe M., 2005. Physicochemical properties and structures of room temperature ionic liquids. 2. Variation of alkyl chain length in imidazolium cation. *Journal of Physical Chemistry B*, **109(13),** 6103-6110.

Triolo A., Russina O., Bleif H.J., Di Cola E., 2007. Nanoscale Segregation in Room Temperature Ionic Liquids. *The Journal of Physical Chemistry B*, **111(18),** 4641-4644.

Urahata, Sergio M., and Ribeiro Mauro C. C., 2005. Single particle dynamics in ionic liquids of 1-alkyl-3-methylimidazolium cations. *The Journal of Chemical Physics*, **122(2),** 024511-9.

Wang H., Gurau G., and Rogers R.D., 2012. Ionic liquid processing of cellulose. *Chemical Society Reviews*, **41(4),** 1519-1537.

Wang, Yanting, and Voth G.A., 2005. Unique Spatial Heterogeneity in Ionic Liquids. *Journal of the American Chemical Society*, **127(35),** 12192-12193.

Wilkes, J. S. and Zaworotko M.J., 1992. Air and water stable 1-ethyl-3-methylimidazolium based ionic liquids. *Journal of the Chemical Society, Chemical Communications*, **0(13),** 965-967.

Wishart J.F., and Ilya A.S., 2009. The Radiation Chemistry of Ionic Liquids and its Implications for their Use in Nuclear Fuel Processing. *In* Ionic Liquids: From Knowledge to Application. Pp. 119-134. ACS Symposium Series, Vol. 1030: American Chemical Society.

Wishart, J. F., 2009. Energy applications of ionic liquids. *Energy & Environmental Science*, **2(9),** 956.

Wu B., Yamashita Y., Endo T., Takahashi K., Castner EW Jr., 2016. Structure and dynamics of ionic liquids: Trimethylsilylpropyl-substituted cations and bis(sulfonyl)amide anions. *Journal of Chemical Physics*, **145(24)**.

Xiao D., Hines L.G. Jr., Li S., Bartsch R.A., and Quitevis E.L., 2009. Effect of Cation Symmetry and Alkyl Chain Length on the Structure and Intermolecular Dynamics of 1,3-Dialkylimidazolium Bis(trifluoromethanesulfonyl)amide Ionic Liquids. *Journal of Physical Chemistry B*, **113(18),** 6426-6433.

Xiao D., Rajian J.R., Cady A., Li S., Bartsch R.A, and Quitevis E.L., 2007. Nanostructural organization and anion effects on the temperature dependence of the optical Kerr effect spectra of ionic liquids. *Journal of Physical Chemistry B*, **111(18),** 4669-4677.

Xiao D., Rajian J.R., Hines L.H.Jr., Li S., Bartsch R.A., and Quitevis E.L., 2008. Nanostructural Organization and Anion Effects in the Optical Kerr Effect Spectra of Binary Ionic Liquid Mixtures. *Journal of Physical Chemistry B*, **112(42),** 13316-13325.

Yang P., Voth G.A., Xiao D., Hines L.G. Jr., Bartsch R.A., and Quitevis E.L., 2011. Nanostructural organization in carbon disulfide/ionic liquid mixtures: Molecular dynamics simulations and optical Kerr effect spectroscopy. *Journal of Chemical Physics*, **135(3)**.

Yang, Z.Z, Zhao Y.Y., and He L.H., 2011. CO2 chemistry: task-specific ionic liquids for CO2 capture/activation and subsequent conversion. *RSC Advances*, **1(4),** 545-567.

Zhou Jing C., Zhe L., Ai Y.H., 2017. Refractive properties of imidazolium ionic liquids with alanine anion C (n) mim Ala (n=2, 3, 4, 5, 6). *Russian Journal of Physical Chemistry A*, **91(10),** 2044-2051.